

Density slope of the nuclear symmetry energy from the neutron skin thickness of heavy nuclei

Lie-Wen Chen,^{1,2} Che Ming Ko,³ Bao-An Li,⁴ and Jun Xu³

¹*Department of Physics, Shanghai Jiao Tong University, Shanghai 200240, China*

²*Center of Theoretical Nuclear Physics,*

National Laboratory of Heavy Ion Accelerator, Lanzhou 730000, China

³*Cyclotron Institute and Department of Physics and Astronomy,
Texas A&M University, College Station, Texas 77843-3366, USA*

⁴*Department of Physics and Astronomy,
Texas A&M University-Commerce, Commerce, Texas 75429-3011, USA*

(Dated: November 6, 2018)

Abstract

Expressing explicitly the parameters of the standard Skyrme interaction in terms of the macroscopic properties of asymmetric nuclear matter, we show in the Skyrme-Hartree-Fock approach that unambiguous correlations exist between observables of finite nuclei and nuclear matter properties. We find that existing data on neutron skin thickness Δr_{np} of Sn isotopes give an important constraint on the symmetry energy $E_{\text{sym}}(\rho_0)$ and its density slope L at saturation density ρ_0 . Combining these constraints with those from recent analyses of isospin diffusion and double neutron/proton ratio in heavy-ion collisions at intermediate energies leads to a more stringent limit on L approximately independent of $E_{\text{sym}}(\rho_0)$. The implication of these new constraints on the Δr_{np} of ^{208}Pb as well as the core-crust transition density and pressure in neutron stars is discussed.

PACS numbers: 21.65.Ef, 21.10.Gv, 26.60.Gj, 21.30.Fe

I. INTRODUCTION

The nuclear symmetry energy $E_{\text{sym}}(\rho)$ that encodes the energy related to the neutron-proton asymmetry in the equation of state (EOS) of isospin asymmetric nuclear matter (ANM) plays a crucial role in both nuclear physics and astrophysics [1–6]. It is also relevant to some interesting issues regarding possible new physics beyond the standard model [7–10]. Although significant progress has been made in recent years in determining the density dependence of $E_{\text{sym}}(\rho)$ [5, 6], large uncertainties still exist even around the normal density ρ_0 . For instance, while the value of $E_{\text{sym}}(\rho_0)$ is determined to be around 30 ± 4 MeV mostly from analyzing nuclear masses, the extracted density slope L of $E_{\text{sym}}(\rho)$ at ρ_0 scatters in a very large range from about 20 to 115 MeV depending on the observables and methods used in the studies [11–13]. Since many observables in terrestrial laboratory experiments intrinsically depend on both $E_{\text{sym}}(\rho_0)$ and L , the extraction of L at an accuracy required for understanding more precisely many important properties of neutron stars [3, 14] is still severely prohibited, although the uncertainty of $E_{\text{sym}}(\rho_0)$ is relatively small. To extract L with higher accuracy is thus of crucial importance.

Theoretically, studies based on both mean-field theories [15–21] and droplet-type models [22–25] have shown that the neutron skin thickness $\Delta r_{np} = \langle r_n^2 \rangle^{1/2} - \langle r_p^2 \rangle^{1/2}$ of heavy nuclei, given by the difference of their neutron and proton root-mean-squared radii, provides a good probe of $E_{\text{sym}}(\rho)$. In particular, Δr_{np} has been found to correlate strongly with both $E_{\text{sym}}(\rho_0)$ and L in microscopic mean-field calculations [15–21] using different parameter sets for the nuclear effective interactions, which all fit the binding energies and charge radii of finite nuclei but correspond to different $E_{\text{sym}}(\rho)$ and give different Δr_{np} . It is, however, difficult to extract an accurate value for L from comparing calculated Δr_{np} of heavy nuclei with experimental data as Δr_{np} depends on a number of nuclear interaction parameters in a highly correlated manner [17, 18] and the calculations have been usually carried out by varying simultaneously the interaction parameters. Similar difficulties also exist when one tries to extract other physical quantities from observables of finite nuclei within mean-field theories or density functional theories [26]. A well-known example is the Skyrme-Hartree-Fock (SHF) approach using normally 9 interaction parameters. Although experimental data on nucleon-nucleon scatterings and properties of both finite nuclei and infinite nuclear matter would in principle put strong constraints on the combinations of these parameters [19, 27–32],

there is generally no constraint on most of the individual interaction parameters. Instead of varying directly the 9 interaction parameters within the SHF, we propose here an alternative approach based on a modified Skyrme-Like (MSL) model [33] to express them explicitly in terms of 9 macroscopic observables that are either experimentally well constrained or empirically well known. This opens the possibility to explore transparently the correlations between properties of finite nuclei and the macroscopic properties of nuclear matter within the SHF approach. In the present work, we use this method to study the correlation between Δr_{np} and various macroscopic observables of infinite nuclear matter by varying individually the values of the latter within their known ranges. We then demonstrate that existing Δr_{np} data on Sn isotopes can give important constraints on L and $E_{\text{sym}}(\rho_0)$. Combining these constraints with those from recent analyses of isospin diffusion and double neutron/proton ratio in heavy-ion collisions at intermediate energies [11], we further show that a more stringent limit on L is obtained approximately independent of the value of $E_{\text{sym}}(\rho_0)$. Finally, we discuss the implication of these new constraints on both the Δr_{np} of ^{208}Pb and the core-crust transition density and pressure in neutron stars.

II. THE THEORETICAL MODEL

In the present work, we use the so-called standard Skyrme interaction (see, e.g., Ref. [34]), which has been shown to be very successful in describing the structure of finite nuclei, especially global properties such as binding energies and charge radii, although non-standard extension is possible [34]. In the standard SHF model, the total energy density of a nucleus is written as [34]

$$\mathcal{H} = \mathcal{K} + \mathcal{H}_0 + \mathcal{H}_3 + \mathcal{H}_{eff} + \mathcal{H}_{fin} + \mathcal{H}_{SO} + \mathcal{H}_{sg} + \mathcal{H}_{Coul} \quad (1)$$

where $\mathcal{K} = \frac{\hbar^2}{2m}\tau$ is the kinetic-energy term and \mathcal{H}_{Coul} is the Coulomb term, and \mathcal{H}_0 , \mathcal{H}_3 , \mathcal{H}_{eff} , \mathcal{H}_{fin} , \mathcal{H}_{SO} , \mathcal{H}_{sg} are given by

$$\mathcal{H}_0 = t_0[(2 + x_0)\rho^2 - (2x_0 + 1)(\rho_p^2 + \rho_n^2)]/4 \quad (2)$$

$$\mathcal{H}_3 = t_3\rho^\sigma[(2 + x_3)\rho^2 - (2x_3 + 1)(\rho_p^2 + \rho_n^2)]/24 \quad (3)$$

$$\begin{aligned} \mathcal{H}_{eff} = & [t_2(2x_2 + 1) - t_1(2x_1 + 1)](\tau_n\rho_n + \tau_p\rho_p)/8 \\ & + [t_1(2 + x_1) + t_2(2 + x_2)]\tau\rho/8 \end{aligned} \quad (4)$$

$$\begin{aligned} \mathcal{H}_{fin} = & [3t_1(2 + x_1) - t_2(2 + x_2)](\nabla\rho)^2/32 \\ & - [3t_1(2x_1 + 1) + t_2(2x_2 + 1)] \\ & \times [(\nabla\rho_n)^2 + (\nabla\rho_p)^2]/32 \end{aligned} \quad (5)$$

$$\mathcal{H}_{SO} = W_0[\vec{J} \cdot \vec{\nabla}\rho + \vec{J}_p \cdot \vec{\nabla}\rho_p + \vec{J}_n \cdot \vec{\nabla}\rho_n]/2 \quad (6)$$

$$\begin{aligned} \mathcal{H}_{sg} = & (t_1 - t_2)[J_p^2 + J_n^2]/16 \\ & - (t_1x_1 + t_2x_2)J^2/16 \end{aligned} \quad (7)$$

in terms of the 9 Skyrme interaction parameters σ , $t_0 - t_3$, $x_0 - x_3$, and the spin-orbit coupling constant W_0 . In the above equations, ρ_i , τ_i and \vec{J}_i are, respectively, the local nucleon number, kinetic energy and spin densities, whereas ρ , τ and \vec{J} are corresponding total densities.

In the MSL model, the EOS of symmetric nuclear matter (SNM) and the nuclear symmetry energy $E_{\text{sym}}(\rho)$ can be expressed, respectively, as [33]

$$E_0(\rho) = E_{\text{kin}}^0 u^{2/3} + Cu^{5/3} + \alpha u/2 + \beta u^\gamma/(\gamma + 1), \quad (8)$$

$$E_{\text{sym}}(\rho) = E_{\text{sym}}^{\text{kin}}(\rho_0)u^{2/3} + Du^{5/3} + E_{\text{sym}}^{\text{loc}}(\rho) \quad (9)$$

where $u = \rho/\rho_0$ is the reduced density; E_{kin}^0 and $E_{\text{sym}}^{\text{kin}}$ are, respectively, the kinetic energy at ρ_0 and its contribution to $E_{\text{sym}}(\rho)$; and $E_{\text{sym}}^{\text{loc}}(\rho)$ is the local density-dependent symmetry energy given by

$$E_{\text{sym}}^{\text{loc}}(\rho) = (1 - y)E_{\text{sym}}^{\text{loc}}(\rho_0)u + yE_{\text{sym}}^{\text{loc}}(\rho_0)u^\gamma \quad (10)$$

with the dimensionless parameter

$$y = \frac{L - 3E_{\text{sym}}(\rho_0) + E_{\text{sym}}^{\text{kin}}(\rho_0) - 2D}{3(\gamma - 1)E_{\text{sym}}^{\text{loc}}(\rho_0)}. \quad (11)$$

The model also includes following density-gradient term in the interaction part of the binding energies for finite nuclei

$$E_{\text{grad}} = G_S(\nabla\rho)^2/(2\rho) - G_V [\nabla(\rho_n - \rho_p)]^2/(2\rho), \quad (12)$$

where G_S and G_V are the gradient and symmetry-gradient coefficients [28].

By comparing expressions (8), (9), and (12) in the MSL model with corresponding ones in SHF, the 9 Skyrme interaction parameters in Eqs. (2)-(7) can be related to the 9 parameters $\alpha, \beta, \gamma, C, D, E_{\text{sym}}^{\text{loc}}(\rho_0), y, G_S$ and G_V in the MSL model by following analytic relations

$$t_0 = 4\alpha/(3\rho_0) \quad (13)$$

$$x_0 = 3(y - 1)E_{\text{sym}}^{\text{loc}}(\rho_0)/\alpha - 1/2 \quad (14)$$

$$t_3 = 16\beta/[\rho_0^\gamma(\gamma + 1)] \quad (15)$$

$$x_3 = -3y(\gamma + 1)E_{\text{sym}}^{\text{loc}}(\rho_0)/(2\beta) - 1/2 \quad (16)$$

$$t_1 = 20C/[9\rho_0(k_{\text{F}}^0)^2] + 8G_S/3 \quad (17)$$

$$t_2 = \frac{4(25C - 18D)}{9\rho_0(k_{\text{F}}^0)^2} - \frac{8(G_S + 2G_V)}{3} \quad (18)$$

$$x_1 = \left[12G_V - 4G_S - \frac{6D}{\rho_0(k_{\text{F}}^0)^2} \right] / (3t_1) \quad (19)$$

$$x_2 = \left[20G_V + 4G_S - \frac{5(16C - 18D)}{3\rho_0(k_{\text{F}}^0)^2} \right] / (3t_2) \quad (20)$$

$$\sigma = \gamma - 1 \quad (21)$$

with $k_{\text{F}}^0 = (1.5\pi^2\rho_0)^{1/3}$. Since the 7 parameters $\alpha, \beta, \gamma, C, D, E_{\text{sym}}^{\text{loc}}(\rho_0)$ and y in the MSL model can be expressed analytically in terms of the 7 macroscopic quantities $\rho_0, E_0(\rho_0)$, the incompressibility K_0 , the isoscalar effective mass $m_{s,0}^*$, the isovector effective mass $m_{v,0}^*$, $E_{\text{sym}}(\rho_0)$, and L [33], the 9 Skyrme interaction parameters $\sigma, t_0 - t_3, x_0 - x_3$ can also be expressed analytically in terms of the 9 macroscopic quantities $\rho_0, E_0(\rho_0), K_0, m_{s,0}^*, m_{v,0}^*, E_{\text{sym}}(\rho_0), L, G_S$, and G_V via above relations.

As a reference for the correlation analyses below, we use following default values for the macroscopic quantities. For the 7 bulk properties of ANM, we take $\rho_0 = 0.16 \text{ fm}^{-3}$, $E_0(\rho_0) = -16 \text{ MeV}$, $K_0 = 230 \text{ MeV}$, $m_{s,0}^* = 0.8m$, $m_{v,0}^* = 0.7m$, $E_{\text{sym}}(\rho_0) = 30 \text{ MeV}$, and $L = 60 \text{ MeV}$. Empirically, values of the gradient coefficient G_S and the symmetry-gradient coefficient G_V are poorly known, although they can be constrained by the nuclear surface energy coefficient a_S , the Landau parameters for the spin and spin-isospin channels

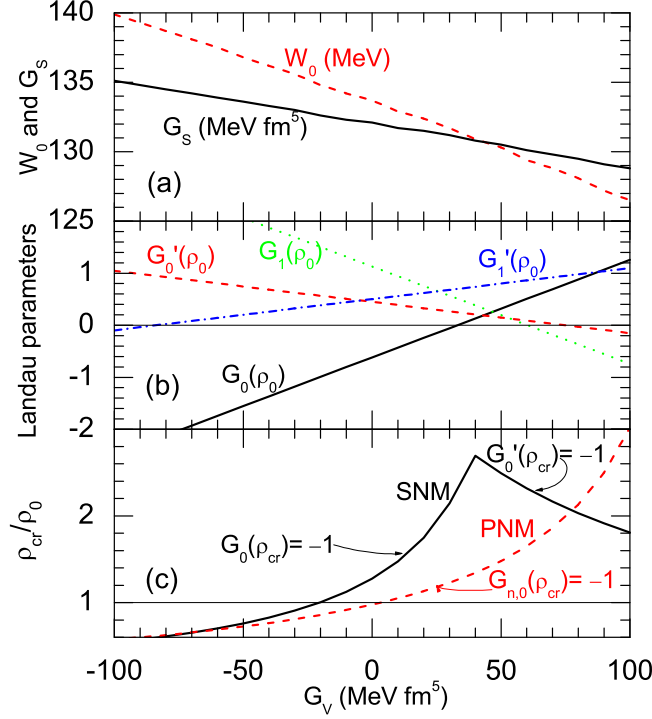


FIG. 1: (Color online) The symmetry-gradient coefficient G_V dependence of G_S and W_0 (a), Landau parameters $G_0(\rho_0)$, $G'_0(\rho_0)$, $G_1(\rho_0)$, $G'_1(\rho_0)$ (b), and the reduced critical density ρ_{cr}/ρ_0 for symmetric nuclear matter and pure neutron matter (c).

in symmetric nuclear matter at the saturation density, i.e., $G_0(\rho_0)$, $G'_0(\rho_0)$, $G_1(\rho_0)$ and $G'_1(\rho_0)$, and the stability condition of nuclear matter [31, 32]. For the existing standard Skyrme parameter sets, we have roughly $G_S = 110 \sim 150 \text{ MeV}\cdot\text{fm}^5$ and $G_V = -40 \sim 40 \text{ MeV}\cdot\text{fm}^5$. Here we use the empirical value of the surface energy coefficient $a_S = 18 \text{ MeV}$ [22] to determine G_S . We note that the surface energy coefficient a_S also depends on the spin-orbit coupling constant W_0 [31, 32, 35] that can be determined by the neutron $p_{1/2} - p_{3/2}$ splitting in ^{16}O . Since the latter depends on G_S and G_V , the three quantities G_S , G_V , and W_0 need to be determined simultaneously.

Keeping the 7 bulk properties of ANM unchanged, we plot in Fig. 1 (a) G_S and W_0 as functions of G_V with the values of G_S , W_0 , and G_V simultaneously giving the surface energy coefficient $a_S = 18 \text{ MeV}$ and fitting the neutron $p_{1/2} - p_{3/2}$ splitting in ^{16}O . In Figs. 1 (b) and (c), we further show the G_V dependence of the Landau parameters $G_0(\rho_0)$, $G'_0(\rho_0)$, $G_1(\rho_0)$, $G'_1(\rho_0)$, and the critical density ρ_{cr} above which at least one Landau parameter violates the stability condition for symmetric nuclear matter and pure neutron matter. Requiring the ρ_{cr}

TABLE I: Skyrme parameters in MSL0 (left side) and some corresponding nuclear properties (right side).

Quantity	MSL0	Quantity	MSL0
t_0 (MeV·fm ³)	-2118.06	ρ_0 (fm ⁻³)	0.16
t_1 (MeV·fm ⁵)	395.196	E_0 (MeV)	-16.0
t_2 (MeV·fm ⁵)	-63.9531	K_0 (MeV)	230.0
t_3 (MeV·fm ^{3+3σ})	12857.7	$m_{s,0}^*/m$	0.80
x_0	-0.0709496	$m_{v,0}^*/m$	0.70
x_1	-0.332282	$E_{\text{sym}}(\rho_0)$ (MeV)	30.0
x_2	1.35830	L (MeV)	60.0
x_3	-0.228181	G_S (MeV·fm ⁵)	132.0
σ	0.235879	G_V (MeV·fm ⁵)	5.0
W_0 (MeV·fm ⁵)	133.3	$G'_0(\rho_0)$	0.42

of symmetric nuclear matter to be larger than ρ_0 leads to $G_V \gtrsim -20$ MeV·fm⁵ and putting $\rho_{cr} > \rho_0$ for pure neutron matter further leads to $G_V \gtrsim 5$ MeV·fm⁵. Empirically, the Landau parameter G'_0 has been extensively investigated, and its value can vary from about zero to 1.6 depending on the models and methods [32, 36–42]. In the present work with the standard SHF approach, a positive G'_0 leads to $G_V \lesssim 70$ MeV·fm⁵ as shown in Fig. 1 (b). Furthermore, the Landau parameter G'_0 can be extracted from the spin-isospin response in finite nuclei, and its value has been found to be 0.45 ± 0.06 in the standard SHF approach [43, 44]. Therefore, we choose here $G_V = 5$ MeV·fm⁵ which leads to $G'_0 = 0.42$, $G_S = 132$ MeV·fm⁵, and $W_0 = 133.3$ MeV·fm⁵. It is interesting to see that the value $G_S = 132$ MeV·fm⁵ is quite consistent with that used extensively in the literature [14, 23, 45]. This new Skyrme parameter set obtained with above empirical values for the macroscopic quantities is referred as MSL0. Summarized in Table I are values of corresponding Skyrme parameters and some macroscopic quantities.

To test the new Skyrme parameter set MSL0, we calculate the binding energies and charge rms radii for a number of closed-shell or semi-closed-shell nuclei: ¹⁶O, ⁴⁰Ca, ⁴⁸Ca, ⁵⁶Ni, ⁷⁸Ni, ⁹⁰Zr, ¹⁰⁰Sn, ¹³²Sn, and ²⁰⁸Pb. Figure 2 shows the relative deviation of the charge rms radii and binding energies of these nuclei from those measured in experiments [46–48].

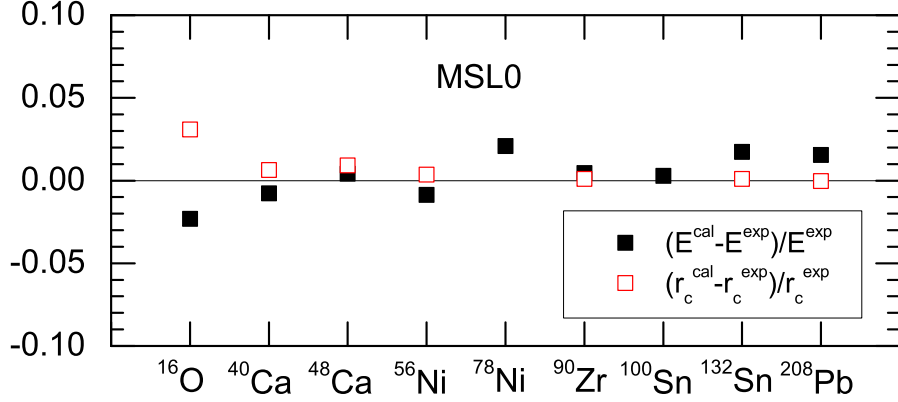


FIG. 2: (Color online) Relative deviation of the binding energies and charge rms radii of ^{16}O , ^{40}Ca , ^{48}Ca , ^{56}Ni , ^{78}Ni , ^{90}Zr , ^{100}Sn , ^{132}Sn , and ^{208}Pb from SHF with MSL0.

It is seen that the MSL0 can describe the experimental data very well except for the light nucleus ^{16}O for which the deviation reaches to about 2 – 3%. This is a remarkable result as MSL0 is not obtained from fitting measured binding energies and charge rms radii of finite nuclei as in usual Skyrme parametrization. It should be pointed out that our main motivation for introducing the MSL0 is not to construct another Skyrme parameter set to describe data, but to use as a reference for the correlation analyses in the following. As we will show, varying G_S , G_V and W_0 will not affect the conclusion in the present work.

III. RESULTS

To reveal clearly the dependence of Δr_{np} on each macroscopic quantity, we vary one quantity at a time while keeping all others at their default values in MSL0. Shown in Fig. 3 are the values of Δr_{np} for ^{208}Pb , ^{120}Sn and ^{48}Ca . Within the uncertain ranges considered here, the Δr_{np} of ^{208}Pb and ^{120}Sn exhibits a very strong correlation with L . However, it depends only moderately on $E_{\text{sym}}(\rho_0)$ and weakly on $m_{s,0}^*$. On the other hand, the Δr_{np} of ^{48}Ca displays a much weaker dependence on both L and $E_{\text{sym}}(\rho_0)$. Instead, it depends moderately on G_V and W_0 . This explains the weaker $\Delta r_{np}-E_{\text{sym}}(\rho)$ correlation observed for ^{48}Ca in previous SHF calculations using different interaction parameters [20]. These results demonstrate that the Δr_{np} of heavy nuclei can provide reliable information on the symmetry energy around the normal density.

As we vary one of the macroscopic quantities in Fig. 3, it is of interest to see how this

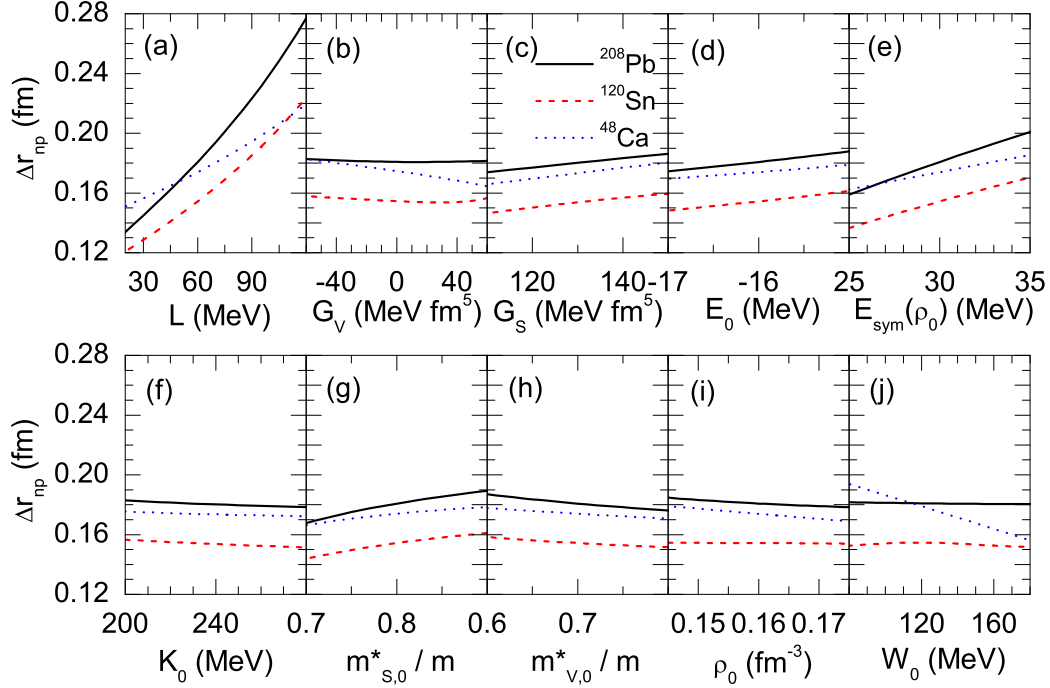


FIG. 3: (Color online) The neutron skin thickness Δr_{np} of ^{208}Pb , ^{120}Sn and ^{48}Ca from SHF with MSL0 by varying individually L (a), G_V (b), G_S (c), $E_0(\rho_0)$ (d), $E_{\text{sym}}(\rho_0)$ (e), K_0 (f), $m_{s,0}^*$ (g), $m_{v,0}^*$ (h), ρ_0 (i), and W_0 (j).

affects the binding energy and charge rms radius. This is shown in Fig. 4 and Fig. 5, respectively, for the changes in the relative deviation of the binding energies and charge rms radii of ^{208}Pb , ^{120}Sn and ^{48}Ca from the data. Within the uncertain ranges for the macroscopic quantities considered here, it is seen that the relative deviation of the binding energy is basically less than 3% except the case for the macroscopic quantity E_0 . For the charge rms radius, the relative deviation is even much smaller. Especially, for the heavy ^{208}Pb and ^{120}Sn , the relative deviation of the charge rms radius is basically less than 0.5% except the case for the macroscopic quantity ρ_0 . These features imply that the binding energies and charge rms radii of finite nuclei can be reasonably reproduced when we perform the correlation analysis shown in Fig. 3 by varying individually the macroscopic quantity. This is particularly the case when we only change the macroscopic quantities L and $E_{\text{sym}}(\rho_0)$ from the MSL0 in the correlation analyses.

Experimentally, much effort has been devoted to determining the values of Δr_{np} for finite nuclei using various methods. In particular, the Δr_{np} of heavy Sn isotopes has been sys-

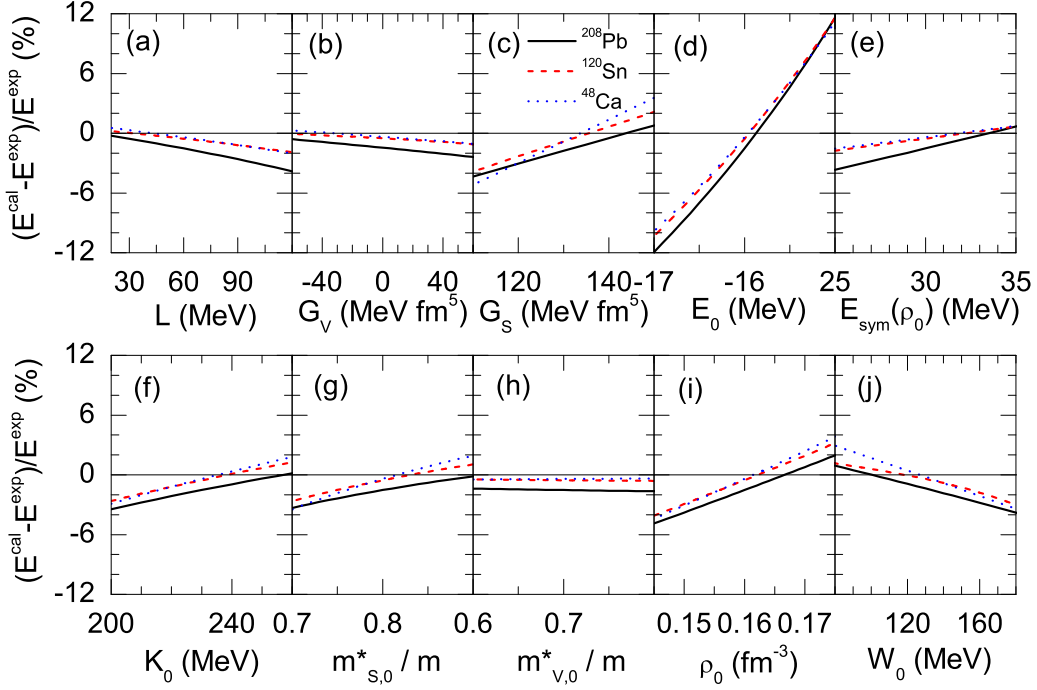


FIG. 4: (Color online) Relative deviation of the binding energies of ^{208}Pb , ^{120}Sn and ^{48}Ca from SHF with MSL0 by varying individually L (a), G_V (b), G_S (c), $E_0(\rho_0)$ (d), $E_{\text{sym}}(\rho_0)$ (e), K_0 (f), $m_{s,0}^*$ (g), $m_{v,0}^*$ (h), ρ_0 (i), and W_0 (j).

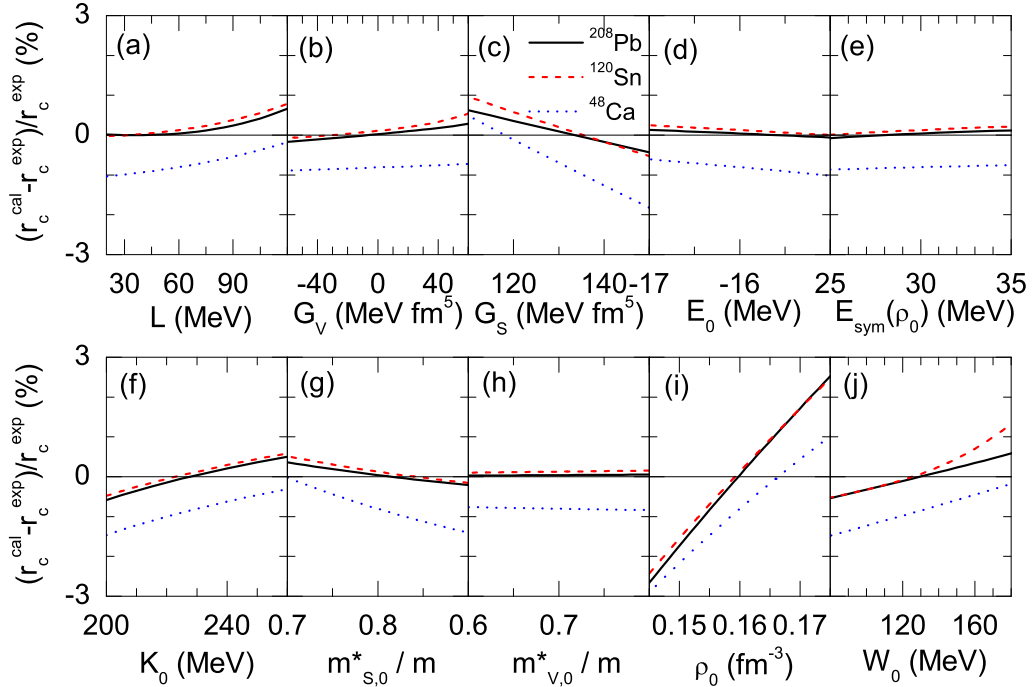


FIG. 5: (Color online) Same as Fig. 4 but for the charge rms radii.

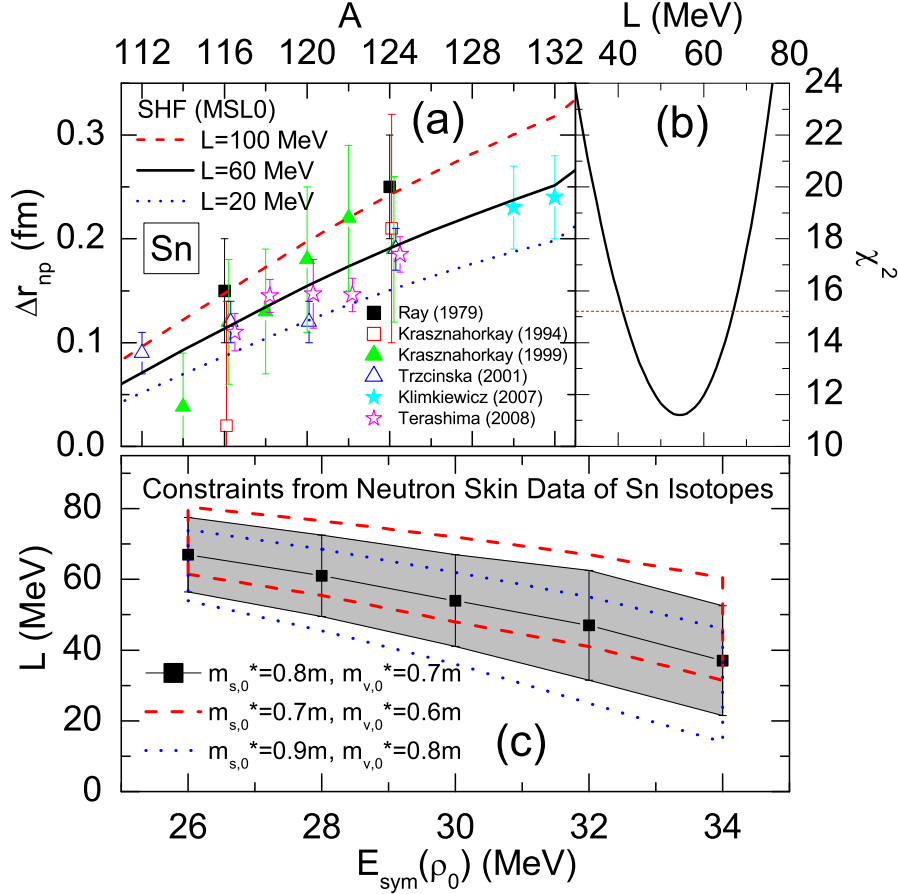


FIG. 6: (Color online) (a): The Δr_{np} data for Sn isotopes from different experimental methods and results from SHF calculation using MSL0 with $L = 20, 60$ and 100 MeV. (b): χ^2 as a function of L . (c): Constraints on L and $E_{\text{sym}}(\rho_0)$ from the χ^2 analysis of the Δr_{np} data on Sn isotopes (Grey band as well as dashed and dotted lines).

tematically measured [49–54]. As an illustration, we first show in Fig. 6 (a) the comparison of available Sn Δr_{np} data with our calculated results using different values of 20, 60 and 100 MeV for L and the default values for all other quantities in MSL0. It is seen that the value $L = 60$ MeV best describes the data. To be more precise, the χ^2 evaluated from the difference between the theoretical and experimental Δr_{np} values is shown as a function of L in Fig. 6 (b). The most reliable value of L is found to be $L = 54 \pm 13$ MeV within a 2σ uncertainty.

Since the value of Δr_{np} depends on both L and $E_{\text{sym}}(\rho_0)$, a two-dimensional χ^2 analysis as shown by the grey band in Fig. 6 (c) is necessary. It is seen that increasing the value of $E_{\text{sym}}(\rho_0)$ systematically leads to smaller values of L . More quantitatively, the value of

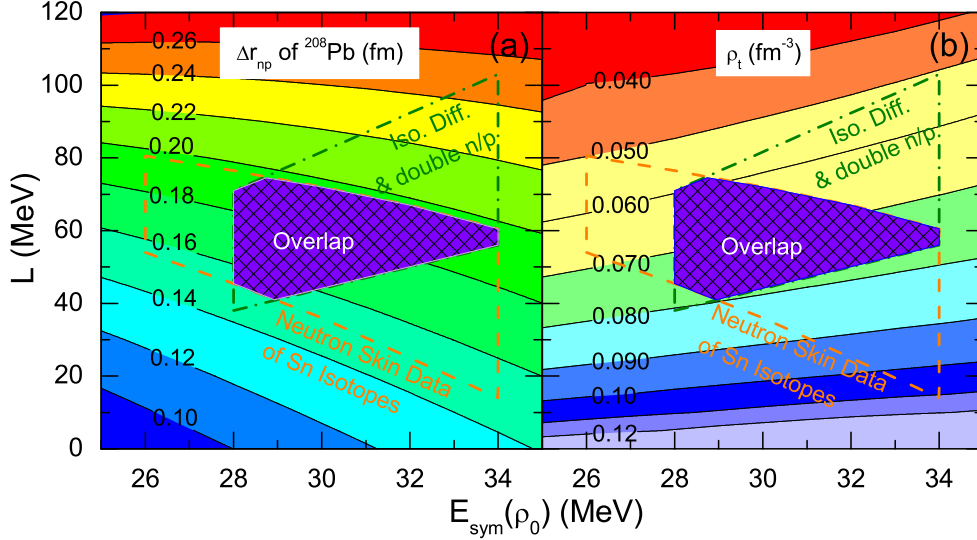


FIG. 7: (Color online) Contour curves in the $E_{\text{sym}}(\rho_0)$ - L plane for the Δr_{np} of ^{208}Pb (a) from SHF calculation with MSL0 and the core-crust transition density ρ_t (b). The shaded region represents the overlap of constraints obtained in the present work (dashed lines) and that from Ref. [11] (dash-dotted lines).

L varies from 67 ± 10.5 to 37 ± 15.5 MeV when the value of $E_{\text{sym}}(\rho_0)$ changes from 26 to 34 MeV. Furthermore, we have estimated the effects of nucleon effective mass by using $m_{s,0}^* = 0.7m$ and $m_{v,0}^* = 0.6m$ as well as $m_{s,0}^* = 0.9m$ and $m_{v,0}^* = 0.8m$, in accord with the empirical constraint $m_{s,0}^* > m_{v,0}^*$ [6, 55], and the resulting constraints are shown by the dashed and dotted lines. As expected from the results shown in Fig. 3, effects of nucleon effective mass are small with the value of L shifting by only a few MeV for a given $E_{\text{sym}}(\rho_0)$. We have also checked that effects of varying other macroscopic quantities are even smaller.

The above constraints on the L - $E_{\text{sym}}(\rho_0)$ correlation can be combined with those from recent analyses of isospin diffusion and double n/p ratio in heavy-ion collisions at intermediate energies [11] to determine simultaneously the values of both L and $E_{\text{sym}}(\rho_0)$. Shown in Fig. 7 (a) (and (b)) are the two constraints in the $E_{\text{sym}}(\rho_0)$ - L plane. Interestingly, these two constraints display opposite L - $E_{\text{sym}}(\rho_0)$ correlations. This allows us to extract a value of $L = 58 \pm 18$ MeV approximately independent of the value of $E_{\text{sym}}(\rho_0)$. This value of L is essentially overlapped with other constraints extracted from different experimental data in the literature [11–13] but with much higher precision although the constraint on $E_{\text{sym}}(\rho_0)$ is not improved. It also agrees well with the value of $L = 66.5$ MeV obtained from a recent

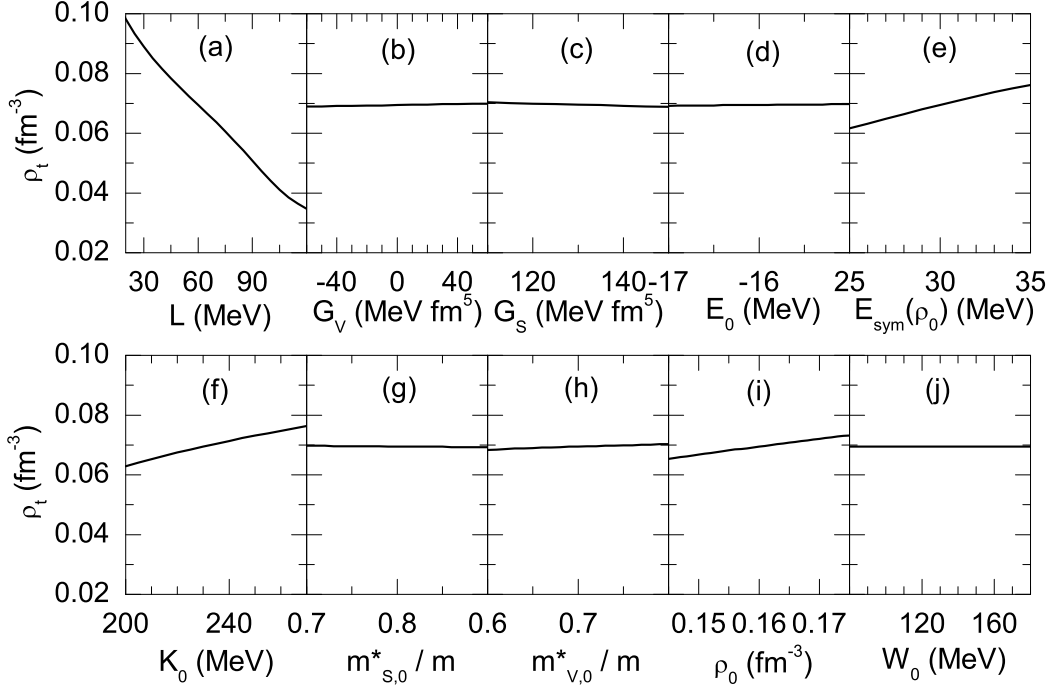


FIG. 8: Same as Fig. 3 but for the core-crust transition density ρ_t in neutron stars.

systematic analysis of the density dependence of nuclear symmetry energy within the microscopic Brueckner-Hartree-Fock approach using the realistic Argonne V18 nucleon-nucleon potential plus a phenomenological three-body force of Urbana type [56]. Furthermore, it is in remarkably good agreement with the value of $L = 52.7$ MeV extracted most recently from global nucleon optical potentials constrained by world data on nucleon-nucleus and (p,n) charge-exchange reactions [57].

Also shown in Fig. 7 (a) are contours of the Δr_{np} of ^{208}Pb . Based on the constraints on L and $E_{\text{sym}}(\rho_0)$ shown by the shaded region in Fig. 7, it is seen that the Δr_{np} of ^{208}Pb is tightly limited to a narrow region of 0.175 ± 0.02 fm, which is quite consistent with other constraints from various experiments [6] but with much smaller uncertainty. The Lead Radius Experiment (PREX) [58] being preformed at Jefferson Lab aims to determine model-independently the $\langle r_n^2 \rangle^{1/2}$ of ^{208}Pb to 1% accuracy, and this is expected to further improve the determination of $E_{\text{sym}}(\rho)$ at subnormal densities.

To see the implications of our results in astrophysics, we have carried out a similar correlation analysis for the transition density ρ_t and corresponding pressure P_t at the inner edge of neutron star crusts, which play crucial roles in neutron star properties [3, 14], using their values evaluated in a dynamical approach [14], and the results are shown in Fig. 8 and

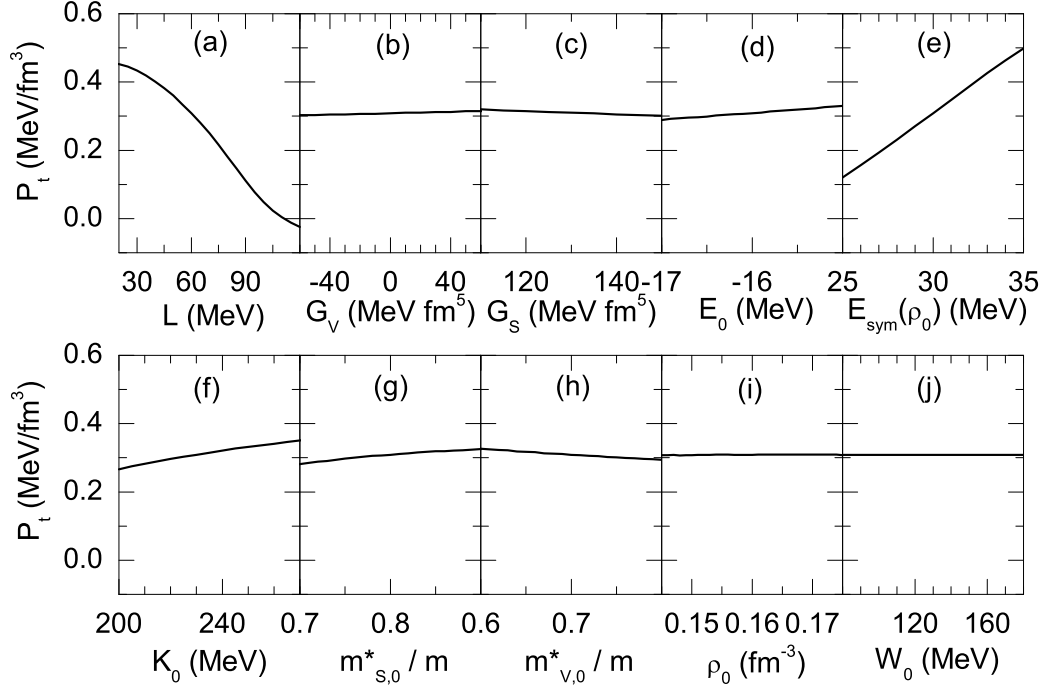


FIG. 9: Same as Fig. 3 but for the the core-crust transition pressure P_t in neutron stars.

Fig. 9, respectively. It is seen that the ρ_t (P_t) displays a particularly strong correlation with L (L and $E_{\text{sym}}(\rho_0)$), a weak dependence on $E_{\text{sym}}(\rho_0)$ and K_0 (K_0), but almost no sensitivity to other macroscopic parameters. These features are consistent with the results in Ref. [14] where ρ_t has been shown to display a stronger correlation with L than P_t in SHF calculations using different interaction parameters. The contours of the core-crust transition density ρ_t in neutron stars in the $E_{\text{sym}}(\rho_0)$ - L plane is shown in Fig. 7 (b). It shows that the value of ρ_t is limited to $0.069 \pm 0.011 \text{ fm}^{-3}$ by the constraints on L and $E_{\text{sym}}(\rho_0)$ obtained in the present work. Including further the uncertainty in the value of K_0 , we obtain a value of $\rho_t = 0.069 \pm 0.018 \text{ fm}^{-3}$. A similar analysis leads to $P_t = 0.33 \pm 0.21 \text{ MeV}/\text{fm}^3$. These results agree well with the empirical values [3] but are slightly larger than previous results in Ref. [14] using $E_{\text{sym}}(\rho_0) = 30.5 \text{ MeV}$ and $L = 86 \pm 25 \text{ MeV}$ extracted only from the isospin diffusion data in heavy-ion collisions [59].

IV. SUMMARY

We have proposed to analyze the correlation between observables of finite nuclei and some macroscopic properties of asymmetric nuclear matter by expressing explicitly the parameters

of the nuclear effective interaction in terms of the macroscopic properties of asymmetric nuclear matter. This would allow us to extract information on some important physical quantities from data on finite nuclei in a more transparent way.

Using such a correlation analysis within the standard SHF approach, we have demonstrated that the neutron skin thickness of heavy nuclei can provide reliable information on the symmetry energy, and the existing neutron skin data on Sn isotopes can give important constraints on the symmetry energy parameters $E_{\text{sym}}(\rho_0)$ and L . In particular, combining the obtained L - $E_{\text{sym}}(\rho_0)$ constraints with that from recent analyses of isospin diffusion and double n/p ratio in heavy-ion collisions has led to a quite accurate value of $L = 58 \pm 18$ MeV approximately independent of the value of $E_{\text{sym}}(\rho_0)$. The obtained L - $E_{\text{sym}}(\rho_0)$ constraints also put a stringent limit of $\Delta r_{np} = 0.175 \pm 0.02$ fm for the neutron skin thickness of ^{208}Pb .

Furthermore, we have explored how the core-crust transition density ρ_t and the corresponding pressure P_t in neutron stars correlate with the macroscopic properties of asymmetric nuclear matter. Our results have indicated that the ρ_t displays a particularly strong correlation with L , a weak dependence on $E_{\text{sym}}(\rho_0)$ and K_0 , but almost no sensitivity to other macroscopic parameters. On the other hand, the P_t exhibits a strong correlation with both L and $E_{\text{sym}}(\rho_0)$, and a weak dependence on K_0 . The L - $E_{\text{sym}}(\rho_0)$ constraints obtained in the present work leads to $\rho_t = 0.069 \pm 0.018$ fm $^{-3}$ and $P_t = 0.33 \pm 0.21$ MeV/fm 3 .

Although we have mainly analyzed in the present work the correlation between the neutron skin thickness of finite nuclei and the symmetry energy within the standard SHF approach, our method can be generalized to other correlation analyses or mean-field models. In particular, it will be interesting to see how our results will change if different energy density functions are used. These studies are in progress.

ACKNOWLEDGMENTS

This work was supported in part by the NNSF of China under Grant No. 10975097, Shanghai Rising-Star Program under Grant No. 06QA14024, the National Basic Research Program of China (973 Program) under Contract No. 2007CB815004 and 2010CB833000, U.S. NSF under Grant No. PHY-0758115 and PHY-0757839, the Welch Foundation under Grant No. A-1358, the Research Corporation under Award No. 7123, the Texas Coordinat-

ing Board of Higher Education Award No. 003565-0004-2007.

- [1] B.A. Li, C.M. Ko, and W. Bauer, *Int. Jour. Mod. Phys. E* **7**, 147 (1998).
- [2] P. Danielewicz, R. Lacey, and W.G. Lynch, *Science* **298**, 1592 (2002).
- [3] J.M. Lattimer and M. Prakash, *Science* **304**, 536 (2004); *Phys. Rep.* **442**, 109 (2007).
- [4] A.W. Steiner, M. Prakash, J.M. Lattimer, and P.J. Ellis, *Phys. Rep.* **411**, 325 (2005).
- [5] V. Baran, M.Colonna, V. Greco, and M. Di Toro, *Phys. Rep.* **410**, 335 (2005).
- [6] B.A. Li, L.W. Chen, and C.M. Ko, *Phys. Rep.* **464**, 113 (2008).
- [7] C.J. Horowitz, S. J. Pollock, P. A. Souder, and R. Michaels, *Phys. Rev. C* **63**, 025501 (2001).
- [8] T. Sil, M. Centelles, X. Viñas, and J. Piekarewicz, *Phys. Rev. C* **71**, 045502 (2005).
- [9] P.G. Krastev and B.A. Li, *Phys. Rev. C* **76**, 055804 (2007).
- [10] D.H. Wen, B.A. Li, and L.W. Chen, *Phys. Rev. Lett.* **103**, 211102 (2009).
- [11] M.B. Tsang, Y. Zhang, P. Danielewicz, M. Famiano, Z. Li, W. G. Lynch, and A. W. Steiner, *Phys. Rev. Lett.* **102**, 122701 (2009).
- [12] A. Carbone, G. Colò, A. Bracco, L.G. Cao, P.F. Bortignon, F. Camera, and O. Wieland, *Phys. Rev. C* **81**, 041301 (R) (2010).
- [13] D.V. Shetty and S.J. Yennello, arXiv:1002.0313v4.
- [14] J. Xu, L.W. Chen, B.A. Li, and H.R. Ma, *Phys. Rev. C* **79**, 035802 (2009); *Astrophys. J.* **697**, 1549 (2009).
- [15] B.A. Brown, *Phys. Rev. Lett.* **85**, 5296 (2000); S. Typel and B.A. Brown, *Phys. Rev. C* **64**, 027302 (2001).
- [16] C.J. Horowitz and J. Piekarewicz, *Phys. Rev. Lett* **86**, 5647 (2001).
- [17] R.J. Furnstahl, *Nucl. Phys.* **A706**, 85 (2002).
- [18] P.-G. Reinhard and W. Nazarewicz, *Phys. Rev. C* **81**, 051303 (2010).
- [19] S. Yoshida and H. Sagawa, *Phys. Rev. C* **69**, 024318 (2004); *ibid.* *C* **73**, 044320 (2006).
- [20] L.W. Chen, C.M. Ko and B.A. Li, *Phys. Rev. C* **72**, 064309 (2005).
- [21] B.G. Todd-Rutel and J. Piekarewicz, *Phys. Rev. Lett* **95**, 122501 (2005).
- [22] W.D. Myers and W.J. Swiatecki, *Ann. Phys.* **55**, 395 (1969); *Nucl. Phys.* **A336**, 267 (1980); *Nucl. Phys.* **A601**, 141 (1996).
- [23] K. Oyamatsu and K. Iida, *Prog. Theor. Phys.* **109**, 631 (2003).

- [24] P. Danielewicz, Nucl. Phys. **A727**, 233 (2003); P. Danielewicz and J. Lee, Nucl. Phys. **A818**, 36 (2009).
- [25] M. Centelles, X. Roca-Maza, X. Viñas, and M. Warda, Phys. Rev. Lett **102**, 122502 (2009); M. Warda, X. Viñas, X. Roca-Maza, and M. Centelles, Phys. Rev. C **80**, 024316 (2009).
- [26] G. Colò, N. Van Giai, J. Meyer, K. Bennaceur, and P. Bonche, Phys. Rev. C **70**, 024307 (2004).
- [27] D. Vautherin and D.M. Brink, Phys. Rev. C **5**, 626 (1972).
- [28] F. Tondeur, M. Brack, M. Farine, and J. M. Pearson, Nucl. Phys. **A420**, 297 (1984).
- [29] P.-G. Reinhard, M. Bender, W. Nazarewicz, and T. Vertse, Phys. Rev. C **73**, 014309 (2006).
- [30] L.G. Cao, U. Lombardo, C.W. Shen, and N. Van Giai, Phys. Rev. C **73**, 014313 (2006).
- [31] J. Margueron, J. Navarro, and N. Van Giai, Phys. Rev. C **66**, 014303 (2002).
- [32] B.K. Agrawal, S. Shlomo and V. Kim Au, Phys. Rev. C **72**, 014310 (2005).
- [33] L.W. Chen, B.J. Cai, C.M. Ko, B.A. Li, C. Shen, and J. Xu, Phys. Rev. C **80**, 014322 (2009).
- [34] E. Chabanat, P. Bonche, P. Haensel, J. Meyer, and R. Schaeffer, Nucl. Phys. **A627**, 710 (1997).
- [35] J. Treiner and H. Krivine, Ann. Phys. **170**, 406 (1986).
- [36] F. Osterfeld, Rev. Mod. Phys. **64**, 491 (1992).
- [37] M. Baldo, U. Lombardo, E.E. Saperstein, and M.V. Zverev, Phys. Lett. **B421**, 8 (1998).
- [38] M. Bender, J. Dobaczewski, J. Engel, and W. Nazarewicz, Phys. Rev. C **65**, 054322 (2002).
- [39] W. Zuo, C.W. Shen, and U. Lombardo, Phys. Rev. C **67**, 037301 (2003).
- [40] C.W. Shen, U. Lombardo, N. Van Giai, and W. Zuo, Phys. Rev. C **68**, 055802 (2003).
- [41] T. Wakasa, M. Ichimura, and H. Sakai, Phys. Rev. C **72**, 067303 (2005).
- [42] I.N. Borzov, Nucl. Phys. **A777**, 645 (2006).
- [43] J. Friedrich and P.-G. Reinhard, Phys. Rev. C **33**, 335 (1986).
- [44] S. Fracasso and G. Colò, Phys. Rev. C **76**, 044307 (2007).
- [45] K. Oyamatsu, I. Tanihata, Y. Sugahara, K. Sumiyoshi, and H. Toki, Nucl. Phys. **A634**, 3 (1998); K. Oyamatsu and K. Iida, Phys. Rev. C **75**, 015801 (2007).
- [46] G. Audi, A.H. Wapstra, and C. Thibault, Nucl. Phys. **A729**, 337 (2003).
- [47] I. Angeli, At. Data Nucl. Data Tab. **87**, 185 (2004).
- [48] F. Le Blanc, L. Cabaret, E. Cottureau, J.E. Crawford, S. Essabaa, J. Genevey, R. Horn, G. Huber, J. Lassen, J.K.P. Lee, G. Le Scornet, J. Lettry, J. Obert, J. Oms, A. Ouchrif, J.

- Pinard, H. Ravn, B. Roussiere, J. Sauvage, and D. Verney, *Phys. Rev. C* **72**, 034305 (2005).
- [49] L. Ray, *Phys. Rev. C* **19**, 1855 (1979).
- [50] A. Krasznahorkay, A. Balanda, J.A. Bordewijk, S. Brandenburg, M.N. Harakeh, N. Kalantar-Nayestanaki, B.M. Nyako, J. Timar, and A. van der Woude, *Nucl. Phys.* **A567**, 521 (1994).
- [51] A. Krasznahorkay, M. Fujiwara, P. van Aarle, H. Akimune, I. Daito, H. Fujimura, Y. Fujita, M.N. Harakeh, T. Inomata, J. Janecke, S. Nakayama, A. Tamii, M. Tanaka, H. Toyokawa, W. Uijen, and M. Yosoi, *Phys. Rev. Lett.* **82**, 3216 (1999).
- [52] A. Trzcinska, J. Jastrzebski, P. Lubiński, F. J. Hartmann, R. Schmidt, T. von Egidy, and B. Klos, *Phys. Rev. Lett.* **87**, 082501 (2001).
- [53] A. Klimkiewicz, N. Paar, P. Adrich, M. Fallot, K. Boretzky, T. Aumann, D. Cortina-Gil, U. Datta Pramanik, Th.W. Elze, H. Emling, H. Geissel, M. Hellstrom, K.L. Jones, J.V. Kratz, R. Kulesa, C. Nociforo, R. Palit, H. Simon, G. Surowka, K. Summerer, D. Vretenar, and W. Walu (LAND Collaboration), *Phys. Rev. C* **76**, 051603 (R) (2007).
- [54] S. Terashima, H. Sakaguchi, H. Takeda, T. Ishikawa, M. Itoh, T. Kawabata, T. Murakami, M. Uchida, Y. Yasuda, M. Yosoi, J. Zenihiro, H.P. Yoshida, T. Noro, T. Ishida, S. Asaji, and T. Yonemura, *Phys. Rev. C* **77**, 024317 (2008).
- [55] T. Lesinski, K. Bennaceur, T. Duguet, and J. Meyer, *Phys. Rev. C* **74**, 044315 (2006).
- [56] I. Vidana, C. Providencia, A. Polls, and A. Rios, *Phys. Rev. C* **80**, 045806 (2009).
- [57] C. Xu, B.A. Li, and L.W. Chen, arXiv:1006.4321v1.
- [58] K. Kumar, R. Michaels, P. A. Souder, and G. M. Urciuoli, spokespersons, <http://hallaweb.jlab.org/parity/prex>.
- [59] L.W. Chen, C.M. Ko, and B.A. Li, *Phys. Rev. Lett.* **94**, 032701 (2005); B.A. Li and L.W. Chen, *Phys. Rev. C* **72**, 064611 (2005).